Acta Cryst. (1996). A**52**, 277–286

Five-Dimensional Symmetry Minimum Function and Maximum-Entropy Method for *Ab Initio* Solution of Decagonal Structures

TORSTEN HAIBACH AND WALTER STEURER

Laboratorium für Kristallographie, ETH Zentrum, 8092 Zurich, Switzerland

(*Received 25 June 1995; accepted 13 October 1995*)

Abstract

A combination of Patterson methods with the maximum-entropy method has been tested for *ab initio* phase determination of decagonal structures. To unravel the n-dimensional Patterson function, the symmetry minimum function, an improvement of the Patterson superposition approach, is extended to the embedding dimensions. This method allows the positions of the hyperatoms to be located and a first crude structure model to be derived. To retrieve the shape and the chemical composition of the perpendicular space component of the hyperatoms, two procedures for applying maximum-entropy methods to phase extension have been derived exclusively constrained by the positions of the hyperatoms in n-dimensional space and the three-dimensional Patterson function. These constraints enforce quasiperiodic solutions with corresponding chemical composition and correct interatomic distances. Applying the maximum-entropy method in perpendicular space allows the decagonal structure to be solved, whereas the physical space approach also provides the capability of determining more complex non-periodic structures as well as deviations from the ideal quasiperiodic structure. Three successful structure solutions of decagonal structures show the potential of this new development.

1. Introduction

Decagonal quasicrystals represent an intermediate state between icosahedral and crystalline phases showing quasiperiodic ordering in two dimensions and periodicity along the third direction. While in the kinematical theory the electron density distribution of periodic structures is related to its structure factors by a simple three-dimensional Fourier transform, quasiperiodic structures need to be embedded in n-dimensional space ($n > 3$) to get an analogous periodic structure-factor equation (Janssen, 1988, and references therein),

$$F(\mathbf{H}) = \sum_{j=1}^{N} \sum_{v=1}^{R_j} f_{jv}(\mathbf{H}) \exp(2\pi i \mathbf{H}\mathbf{x}_j), \qquad (1)$$

where $f_{jv}(\mathbf{H})$ indicates the Fourier transforms of the vth atom type within the jth hyperatom and $\mathbf{x}_j$ its position in an n-dimensional unit cell containing N hyperatoms, each of them consisting of R atom types. The n-dimensional periodic lattice is spanned by the vectors $\mathbf{d}_i$ (D basis) adapted to the symmetry. The corresponding orthogonal n-dimensional space V of the embedded structure can now be separated into two orthogonal subspaces. The three-dimensional parallel space $V^{\parallel}$ is used to describe the quasiperiodic electron-density distribution. The components of the hyperatoms in the $(n-3)$-dimensional perpendicular space $V^{\perp}$, the acceptance domains, generate the quasiperiodic distribution of the atomic sites in the cut-and-project approach. Consequently, the n-dimensional scattering vector $\mathbf{H}$ consists of two main components, $\mathbf{H}^{\parallel}$ and $\mathbf{H}^{\perp}$. One part of the n-dimensional scattering factor $f_{jv}(\mathbf{H})$, the conventional atomic scattering factor $f_{jv}^{\parallel}(\mathbf{H}^{\parallel})$, is the Fourier transform of a single atom of type v in physical space. The other part, the geometric structure factor (Jaric, 1986),

$$f_{jv}^{\perp}(\mathbf{H}^{\perp}) = (1/A^{\perp}) \int \exp(2\pi i \mathbf{H}^{\perp}\mathbf{x}_j^{\perp})\, \mathrm{d}A_{jv}, \qquad (2)$$

represents the Fourier transform of the area A_{jv} of the vth atom type within the acceptance domain A_j of the jth hyperatom normalized to $A^{\perp}$, the n-dimensional unit cell projected onto the perpendicular space. Contrary to conventional crystallographic structure analysis, not only the positions of the hyperatoms $\mathbf{x}_j$ have to be retrieved but also the shape and the detailed structure of the acceptance domains A_j. Consequently, the phase reconstruction consists of two steps: (*a*) finding the positions of the hyperatoms in the n-dimensional unit cell; and (*b*) determining the shape and structure of their acceptance domains.

Attempts to solve this problem have mainly been by trial-and-error methods based on structure models derived from the n-dimensional Patterson function. A first discussion of direct methods in n-dimensional space (Fu, Li & Fan, 1993) has shown that based on a full data set a simulated simple structure could be solved. However, in quasiperiodic substances some of the fundamental assumptions of direct methods are not fulfilled and their use will be limited. For instance, diffraction data of decagonal quasicrystals are in general incomplete and lack atomic resolution, especially in perpendicular space (Steurer, Haibach, Zhang, Kek & Lück, 1993). These data violate the underlying statistical

assumption of data completeness and up to now n-dimensional structure factors cannot be normalised.

In addition, methods based on anomalous scattering as well as contrast variation could be successfully applied in quasiperiodic structure determination to get partial structure factors (deBoissieu *et al.*, 1994). However, these experimental methods are restricted to quasicrystals of suitable chemical composition. Another approach to solve the phase problem is based on known structures of related rational approximants (Jaric & Qiu, 1993) that can be transformed by an n-dimensional shear to the corresponding quasiperiodic one.

2. Structure solution by Patterson and maximum-entropy methods

This paper will focus on an extension and combination of two algorithms in five-dimensional real space: solving the decagonal structure by unravelling the five-dimensional Patterson function and determining the acceptance domains with a restrained maximum-entropy algorithm.

Despite the incompleteness of data sets obtained by X-ray diffraction experiments, cuts through the five-dimensional Patterson function of decagonal structures perpendicular to $V^{\perp}$ show few, but distinct, peaks (Steurer, 1989). Using the embedding method, the infinite number of quasiperiodically ordered atoms condenses to only a few hyperatoms in an n-dimensional unit cell. As most of the decagonal quasicrystals consist of aluminium and transition metals, some hyperatoms with large acceptance domains of transition metals consequently generate interatomic vectors with 'heavy' weight. Hence, their positions can be easily derived from the Patterson function. A systematic analysis of all peaks in the Patterson map with special emphasis on the Harker vectors (Harker, 1936) in the five-dimensional space group will result in all possible positions of hyperatoms in the embedded unit cell.

Unfortunately, data sets of quasicrystals lack resolution in $V^{\perp}$. In consequence, the Patterson peaks are severely broadened in this subspace and the shape of the acceptance domains cannot be found by unravelling the Patterson function. However, if the positions of the hyperatoms are known, the phases of the strong structure factors can be determined. To reconstruct the phases of the weak structure factors and to improve the resolution in $V^{\perp}$, new methods have to be derived. The maximum-entropy method used for image enhancement allows electron-density maps with high resolution to be generated. On the other hand, this method provides the possibility of retrieving the unknown phases and to find a structure solution in agreement with all given restrictions. As the maximum-entropy solution strongly depends on the choice of proper constraints and restraints, it is of great importance to take advantage of the complete prior knowledge. Based on the positions of the hyperatoms, a calculation of the electron density restricted to their acceptance domains will constrain the maximum-entropy method to a quasiperiodic distribution of atoms with distinct distances in physical space. Starting with a trial electron density derived from unravelling the Patterson function, the maximum-entropy solution results in sharp boundaries of the acceptance domains with distinct subdivisions, and a detailed n-dimensional structure solution can be found.

3. Symmetry minimum function and image-seeking minimum function

Owing to the limited resolution of the obtainable Patterson maps, it is necessary to take into account not only the peaks but also the entire Patterson map. A very effective way of unravelling Patterson maps pixelwise is the symmetry minimum function SMF (Estermann, 1995). This function,

$$\mathrm{SMF}(\mathbf{x}) = \min[(1/m_i)P(\mathbf{x} - S_i\mathbf{x})|S_i \in G_{nD}], \quad (3)$$

examines the unique Harker vectors, generated by the symmetry operations S_i of the space group G_{nD} with multiplicity m_i, on a regular grid in the Patterson map $P(\mathbf{U})$. Taking the minimum over all symmetry-equivalent vectors ensures that all atomic positions $\mathbf{x}$ incompatible with the corresponding Cheshire group (Hirshfeld, 1968) are assigned to the background value (Simpson, Dobrott & Lipscomb, 1965). Hence, only positions in accord with the space-group symmetry will remain.

3.1. *Symmetry minimum function in decagonal space groups*

Based on the point symmetry of the reciprocal space and systematic extinctions, quasiperiodic structures can be assigned to n-dimensional space groups (Mermin, 1992). The most common decagonal space group is $P10_5/mmc$, which has the four generators $\bar{1}$ (0,0,0,0,0), 10_5 (0,0,0,0,x_5), m ($x_1x_2x_2x_1$,x_5) and m (x_1,x_2,x_3,x_4,1/4). Given a general position ($x_1x_2x_3x_4x_5$), the most important of all 32 unique Harker vectors ($u_1u_2u_3u_4u_5$) and their multiplicities m_i are listed below (Table 1). No matter how broad the Harker peaks ($2x_12x_22x_32x_42x_5$) are, positions ($x_1x_2x_3x_4x_5$) will be significant only if all of the corresponding Harker vectors are above background level. However, the solution of the symmetry minimum function belongs to the Cheshire group, the Euclidean normalizer of the five-dimensional space group, and will show some ambiguities: the enantiomorph structure as well as all structures related by a permissible origin shift, *e.g.* (0,0,0,0,1/2) in $P10_5/mmc$, are included within the same symmetry minimum map. Considering centrosymmetric decagonal space groups, peaks of the symmetry minimum function generated only by permissible origin shifts can be grouped together and treated as symmetry-equivalent solutions. In consequence, the subsequent

Table 1. *Most important unique Harker vectors and their multiplicities m_i for the space group $P10_5/mmc$*

u_1	u_2	u_3	u_4	u_5	m_i
0	0	0	0	$2x_5$	20
x_1+x_4	$-x_1-x_3-x_4$	x_1+x_3	x_2+x_4	$\frac{1}{2}$	4
$2x_1$	$2x_2$	$2x_3$	$2x_4$	$\frac{1}{2}$	2
$2x_1$	$2x_2$	$2x_3$	$2x_4$	$2x_5$	1

structure analysis will be reduced to one member of each group.

Decagonal structures with quasiperiodic layers derivable from a primitive undecorated five-dimensional hypercubic lattice show in the four-dimensional description only hyperatoms lying on the diagonal of a hyperrhombohedron. Hence, there exists a characteristic section spanned by the diagonal of the four-dimensional hyperrhombohedron $[11110]^P$ and the periodic direction $[00001]^P$ containing all information about the positions of the hyperatoms. The initial five-dimensional problem can therefore be treated in the corresponding two-dimensional subgroup, *e.g.* $P10_5/mmc$ is reduced to *p2mg*. Solving the symmetry minimum function in this plane group reveals all possible positions of the hyperatoms in the characteristic section. Nevertheless, the permissible origin shifts have to be derived from the five-dimensional supergroup. Only a subset of the permissible origin shifts in the two-dimensional space group are related to the corresponding five-dimensional supergroup.

3.2. *Retrieving the positions of the hyperatoms*

By selecting the strongest peak of the symmetry minimum function as a reliable position of a hyperatom, further structural information can be retrieved by choosing its corresponding position $\mathbf{x}^P$ as pivot element. Comparing it pixelwise with all other trial atomic positions $\mathbf{x}$, the interatomic cross vectors $\mathbf{x}-\mathbf{x}^P$ can be searched in the Patterson map. Generating all symmetry-equivalent positions $S_i\mathbf{x}^P$ and taking the minimum over all cross vectors $\mathbf{x}-S_i\mathbf{x}^P$ with the image-seeking minimum function IMF (Estermann, 1995),

$$\mathrm{IMF}(\mathbf{x}) = \min[P(\mathbf{x}-S_i\mathbf{x}^P)|S_i \in G_{nD}], \qquad (4)$$

an unambiguous structure solution can be obtained. As the five-dimensional unit cell consists of a small number of hyperatoms with strong scattering power, selecting the strongest peak in the symmetry minimum function as pivot element will result in a feasible map. In the actual studies, the remaining positions taken as pivot element did not change the solution of the image-seeking minimum function. In the case of non-centrosymmetric decagonal space groups, a second suitable pivot element has to be chosen simultaneously to fix one of the two possible enantiomorph solutions.

As the SMF/IMF algorithm allows the positions of the hyperatoms to be retrieved and small changes in the shape of their acceptance domains mostly affect weak structure factors, those with large amplitude can be assigned their corresponding phases. Modelling the shape of the acceptance domains and selecting all structure factors being invariant allows this phase assignment to be verified. Hence, the structure model attained can be taken as a reliable starting electron-density distribution for a subsequent maximum-entropy analysis.

4. Maximum-entropy solution of acceptance domains

Owing to the reasons mentioned in §2, a further analysis of the acceptance domains has to be carried out by the maximum-entropy method (MEM). In principle, three different direct-space techniques of finding the maximum-entropy solution of decagonal quasicrystals are possible: (*a*) calculation of the density distribution in the five-dimensional unit cell; (*b*) determination of the atomic density distribution only within the two-dimensional acceptance domains; (*c*) determination of the three-dimensional electron-density distribution in parallel space within a box with dimensions corresponding to the coherence length related to the diffraction experiment. For technical reasons, a direct computation of the five-dimensional electron density distribution lacks efficacy and resolution. As the acceptance domains are parallel to $V^\perp$ and in consequence irrational to the five-dimensional lattice as well as to each other, any regular five-dimensional grid allows neither the determination of the acceptance domains in $V^\perp$ nor the electron-density distribution in $V^\parallel$ without interpolation. Using conventional computing facilities, the memory available will thus reduce the resolution in an unacceptable way. Restricting the five-dimensional density distribution to the acceptance domains as determined by the method shown in §3, however, is a very efficacious way of retrieving unknown phases. Representing the quasicrystal in parallel space not only allows the embedded structure to be solved, but also generates an electron-density map in physical space showing no Fourier-series truncation errors, and further physical constraints can be directly included.

4.1. *Basic equations*

Although the theory of solving crystal structures by means of the maximum-entropy method has been extensively discussed (Collins, 1982; Bricogne, 1984; Livesey & Skilling, 1985) and even macromolecular structures can be successfully solved (Bricogne, 1993, and references therein), up to now only one-dimensional quasiperiodic sequences have been analysed in non-periodic systems with special emphasis on the suitability and reliability of the maximum-entropy method

(Papoular, deBoissieu & Janot, 1991). The authors present a profound discussion of the influence of noise and truncation effects in the maximum-entropy solution if all phases of the structure factors are known. A first application of the maximum-entropy method for image enhancement in five-dimensional space was presented by Steurer (1991). The calculation was performed on a hyperrhombohedral grid and the representation of the acceptance domains was obtained by bicubic interpolation. A three-dimensional maximum-entropy algorithm based on known phases was used to generate high-resolution electron-density maps of decagonal $Al_{70}Co_{15}Ni_{15}$ (Steurer *et al.*, 1993).

Solving decagonal structures requires the fundamental maximum-entropy equations (Bricogne, 1984)

$$q_i = \frac{p_i}{Z(\lambda_1, \ldots, \lambda_{N_C})} \exp\left(\sum_{n=1}^{N_c} \lambda_n \frac{\partial C_n}{\partial q_i}\right) \qquad (5)$$

$$Z(\lambda_1, \ldots, \lambda_{N_C}) = \sum_{i=1}^{N_P} p_i \exp\left(\sum_{n=1}^{N_C} \lambda_n \frac{\partial C_n}{\partial q_i}\right) \qquad (6)$$

to be solved in five dimensions for all N_P grid points q_i restricted to all N_C constraint equations C_n by Lagrange multipliers λ_n. Two different constraint equations are necessary to take all structure factors derived from the symmetry minimum solution and all the observed structure amplitudes simultaneously into account. If the noise is assumed to be Gaussian, the known structure factors $F_{obs}(\mathbf{H})$ can be constrained by

$$C_1 = \sum_{\mathbf{H}} (1/\sigma^2) \left|F_{obs}(\mathbf{H}) - F_{clc}(\mathbf{H})\right|^2 = \chi^2 \qquad (7)$$

with their corresponding standard deviations σ. The second constraint equation (*c.f.* Sakata & Sato, 1990) only depends on the structure amplitudes and restrains all unknown phases to

$$C_2 = \sum_{\mathbf{K}} (1/\sigma^2) \left|\left|F_{obs}(\mathbf{K})\right| - \left|F_{clc}(\mathbf{K})\right|\right|^2 = \chi^2. \qquad (8)$$

Substituting (7) and (8) into (5) results in a five-dimensional algorithm:

$$\begin{aligned} q_i = [p_i/Z(\lambda_1, \lambda_2)] \exp\Big[& -2\lambda_1 \sum_{\mathbf{H}} (1/\sigma^2) \\ & \times \left|F_{obs}(\mathbf{H}) - F_{clc}(\mathbf{H})\right| \cos(2\pi \mathbf{H}\mathbf{x}_i - \varphi_\Delta) \\ & - 2\lambda_2 \sum_{\mathbf{K}} (1/\sigma^2) \left|\left|F_{obs}(\mathbf{K})\right| - \left|F_{clc}(\mathbf{K})\right|\right| \\ & \times \cos(2\pi \mathbf{K}\mathbf{x}_i - \varphi_{clc}) \Big]. \end{aligned} \qquad (9)$$

with $\varphi_\Delta = \arctan\{\mathrm{Im}[F_{obs}(\mathbf{H}) - F_{clc}(\mathbf{H})]/\mathrm{Re}[F_{obs}(\mathbf{H}) - F_{clc}(\mathbf{H})]\}$, the phase of the structure-factor difference. This equation can be maximized solving λ_i by Newton's method (Bricogne, 1984) or by exponential modelling (Collins & Mahar, 1983). However, using solely the above constraint equations and iterating with the exponential modelling procedure is a very unstable way in finding the global maximum. To obtain a solution that is in agreement with all physical constraints, one has to take into account the interatomic distances and to avoid unphysically shaped atoms. The most feasible solution can be found using as many constraints as possible that are previously known. In the case of quasicrystals, the kind of ordering as well as all possible interatomic distances can be easily constrained by restricting the density calculation onto the planes of the acceptance domains. Separating the five-dimensional space into the two orthogonal subspaces and introducing the geometric structure factor (2), (9) can be rewritten as a pseudo two-dimensional algorithm in $V^\perp$:

$$\begin{aligned} q_i = [p_i/Z(\lambda_1, \lambda_2)] \exp\Big[& -2\lambda_1 \sum_{\mathbf{H}} (\bar{f}^{\parallel}/\sigma^2) \\ & \times \left|F_{obs}(\mathbf{H}) - F_{clc}(\mathbf{H})\right| \cos(2\pi \mathbf{H}^\perp \mathbf{x}_i^\perp + \varphi_i^0 - \varphi_\Delta) \\ & - 2\lambda_2 \sum_{\mathbf{K}} (\bar{f}^{\parallel}/\sigma^2) \left|\left|F_{obs}(\mathbf{K})\right| - \left|F_{clc}(\mathbf{K})\right|\right| \\ & \times \cos(2\pi \mathbf{K}^\perp \mathbf{x}_i^\perp + \varphi_i^0 - \varphi_{clc}) \Big]. \end{aligned} \qquad (10)$$

The maximum-entropy calculation has now to be performed exclusively on a set of two-dimensional planes parallel to $V^\perp$ centred at the positions of the hyperatoms $\mathbf{x}_i^0$ with the corresponding phase

$$\varphi_i^0 = 2\pi \mathbf{H}\mathbf{x}_i^0. \qquad (11)$$

As the atomic distribution is restricted to the planes of the acceptance domains, there exist further inherent constraints. The structure solution will obviously be quasiperiodic and avoiding overlap of acceptance domains introduces the closeness condition (Kalugin & Katz, 1993), *e.g.* only physical atomic distances can be generated. To introduce this constraint, it is proposed that grid points in the planes of the acceptance domains are generated with identical perpendicular components. The sum of the occupancies of adjacent acceptance domains can be limited to unity. Hence, a reliable density distribution on the scale of the average atomic scattering factor $\bar{f}^{\parallel}$ including the overall Debye–Waller factor is derived and the geometric structure factor can be determined. Based on the crude structure model derived by the SMF/IMF algorithm, the remaining unknown phases can be retrieved and a detailed structure solution can be derived.

4.2. *Representation of decagonal quasicrystals in physical space*

The algorithm introduced in §4.1 is an efficient way of solving the phase problem as the problem is reduced to two dimensions. As mentioned above, generating the electron-density distribution in parallel space by using a three-dimensional cut through the five-dimensional

structure lacks resolution, and artefacts caused by interpolation algorithms may be induced. The electron-density distribution can now be obtained by a Fourier transform using the phases solved by the two-dimensional maximum-entropy calculation. However, as Fourier-series truncation errors severely bias this electron-density calculation (*cf.* §2), achieving high resolution in physical space needs a further maximum-entropy computation to be performed. Based on a three-dimensional grid in $V^{\parallel}$, (9) can only be fulfilled exactly if the number of grid points N_P is infinite. The experimentally observed half-widths (FWHM) of the Bragg peaks actually indicate coherence lengths of decagonal quasicrystals of the order of 1000 to 10000 Å. Conventional three-dimensional maximum-entropy calculations show that decagonal structures with lattice parameters $a^D_{1,\ldots,4} \simeq 4$ Å, a^D_5 are reasonably represented by an orthorhombic box with dimensions $a^O_{1,2} \geq 400$ Å, $a^O_3 = a^D_5$ (Haibach, 1994). Using an analogous expression to (9) in three dimensions, the electron-density distribution of the quasicrystal can now be represented on a regular three-dimensional grid. Fixing all phases of the structure factors solved by the procedure discussed in §4.1, the less biased structure of the ideal quasicrystal in physical space can be found.

On the other hand, all quasicrystals observed up to now exhibit a considerable amount of diffuse scattering due to structural disorder (Frey & Steurer, 1993). Solving the maximum-entropy equations in $V^{\perp}$ exclusively around the centres of the hyperatoms is a strong constraint to an ideally perfect quasicrystal. It does not allow any atomic shifts in $V^{\parallel}$ beyond phason flips. In consequence, the above procedure can be only the first crude step in finding an average local building element. For a detailed analysis of the average real structure, a maximum-entropy algorithm in $V^{\parallel}$ will be more suited as it is more variable. Not only intensities at Bragg positions, but also diffuse scattering, can be used as observed data. Hence, the method can be extended to the non-periodic case calculating the entire direct space of a disordered structure using Bragg peaks and diffuse intensities as well. However, there are more structural degrees of freedom. The main constraints in a physical space algorithm are given in (7) and (8) for the set of known phases and known structure amplitudes. To result in a reliable and reproducible maximum of entropy, further restrictions have to be used and all prior knowledge has to be implemented. Instead of creating a construct of constraint equations, however, the Patterson function is a feasible mask for the maximum-entropy algorithm.

4.3. *Using the Patterson function as prior knowledge*

As the Patterson function is the pair correlation function, the atomic positions of the structure have to be a subset of all Patterson peaks. This function can be calculated from the observed intensities without prior knowledge. Hence, a normalized cut of the five-dimensional Patterson function parallel to $V^{\parallel}$ can be considered as prior electron-density distribution. All permissible atomic positions will coincide with a Patterson peak. In consequence, all existing interatomic distances in the structure as well as the global quasiperiodic ordering within the given size of the three-dimensional representation are guaranteed. Maximizing the entropy starting with this prior distribution will cause some of the Patterson peaks to vanish and others to change their relative values. Generating new atomic positions is hindered, however.

Fixing the phases of the strongest reflections will further constrain the maximum-entropy solution to the average structure model consistent with the image-seeking minimum map. In non-centrosymmetric decagonal structures, one has to select special reflections in addition to fix one of the two enantiomorphs. It has to be stressed that fixing the phases derived from the trial five-dimensional structure model can only be correlated with the three-dimensional Patterson map if one of the hyperatoms is situated at the origin. Otherwise, the origin of the structure model has to be shifted.

The resulting electron-density map shows all atomic positions in physical space. Assigning each peak its integrated density, the corresponding atom type is determined and the acceptance domains can be constructed analytically or the atomic positions can individually be lifted in five-dimensional space. For the latter procedure, each atomic position is described on the five-dimensional orthogonal basis V as $\mathbf{x}^{\parallel} = (x_1 x_2 x_3 000)^T$. If these vectors are transformed onto the basis D with basis vectors $\mathbf{d}_i$, they can be shifted back into one unit cell

$$\mathbf{x}^V_{\text{red}} = W^{-1} \bmod(W\mathbf{x}^{\parallel}, \mathbf{d}_i) \qquad (12)$$

with the matrix W that transforms the coordinates of the V basis to the D basis.

With the atomic positions corresponding to the same hyperatom accumulated, the acceptance domains can be redrawn by a simple back transformation onto the basis V considering cuts parallel to $V^{\perp}$. Hence, the physical-space maximum-entropy solution can easily be described in the n-dimensional approach and a subsequent least-squares refinement allows the final structure model to be verified.

5. Results

The reliability and efficacy of the algorithms presented above were first tested using a hypothetical structure similar to decagonal $Al_{70}Co_{15}Ni_{15}$ with pentagrammal acceptance domains (Fig. 1) consisting of $Al_{53}Ni_{15}Rh_{33}$. The influence of the size of the parallel-space representation of the resolution of data sets and of the density of grid points was extensively studied. These parameters

were determined empirically. The minimum conditions that guarantee a correct but rather biased solution (grid effects: sharp and distorted electron-density distribution of atoms) as well as the optimum conditions (correct and less biased structure, smooth electron-density distribution) are given in Table 2. Comparison of the lifted Fourier map (Fig. 2) and the lifted maximum-entropy map (Fig. 3), both calculated on a data set with $|\mathbf{H}^{\perp}| \leq 1.0\,\text{Å}^{-1}$ (136 reflections in the zeroth layer), shows the improved resolution of the latter method impressively. The structured point distribution in the acceptance domain obtained by lifting the atoms refers to the limited size of the parallel-space region. The radius of each point represents the integrated electron density of the lifted atomic types. The large dots correspond to rhodium, the medium dots to nickel and the small dots to aluminium.

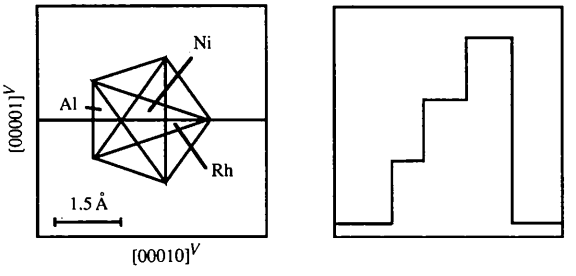

Fig. 1. (*a*) Pentagrammal acceptance domain of hypothetical decagonal $Al_{53}Ni_{15}Rh_{32}$ corresponding to hyperatom 2 of $Al_{70}Co_{15}Ni_{15}$ (Steurer *et al.*, 1993). (*b*) Section through the acceptance domain along the line drawn in (*a*).

Table 2. *Minimum and optimum parameters for the $V^{\parallel}$-MEM calculation*

a_i^O: orthorhombic box dimensions; a_i^D: decagonal lattice parameters (V basis)

Parameters	Minimum	Optimum
Parallel-space region	$a_{1,2}^O \geq 100\lvert a_{1,\ldots,4}^D\rvert$, $a_3^O = d_5^D$	$a_{1,2}^O \geq 400\lvert d_{1,\ldots,4}^D\rvert$, $a_3^O = a_5^D$
Grid resolution (Å)	0.19	0.10
Data-set resolution in $V^{\perp}$ (Å^{-1})	$\lvert\mathbf{H}^{\perp}\rvert \geq 1.0$	$\lvert\mathbf{H}^{\perp}\rvert \geq 2.0$

The lowest densities plotted refer to an integral density of one hundredth of the maximum in the maximum-entropy solution, whereas concerning the Fourier transform the cut-off level has been increased to 15% (half-occupied aluminium position) for clarity. Despite the fact that low occupancy and chemical disorder were not prohibited, the map generated with the maximum-entropy algorithm shows a very sharp contrast corresponding to the regions of different chemical composition. One can clearly distinguish the pentagrammal regions of the trial structure.

5.1. *The structure solution of $Al_{70}Ci_{15}Ni_{15}$*

Decagonal $Al_{70}Co_{15}Ni_{15}$ provided a good test example for the combined use of the symmetry minimum function and the maximum-entropy method. It has a five-dimensional unit cell with $d_{1,\ldots,4} = 3.393\,(1)$, $d_5 = 4.0807\,(3)$ Å, $\alpha_{ij} = 60$, $\alpha_{i5} = 90°$ $(i, j = 1, \ldots 4)$, space group $P10_5/mmc$, and the structure is known (Steurer *et al.*, 1993). The actual data set was recently collected at the synchrotron facility HASYLAB at

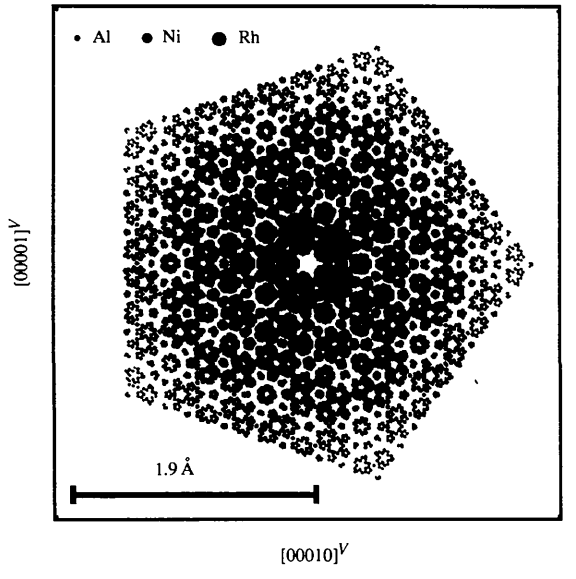

Fig. 2. Simulated structure: acceptance domain of hyperatom 1 calculated with a Fourier transform in $V^{\parallel}$ (760 × 760 Å) lifted in $V^{\perp}$ (cut-off limit: 15% ρ_{max}).

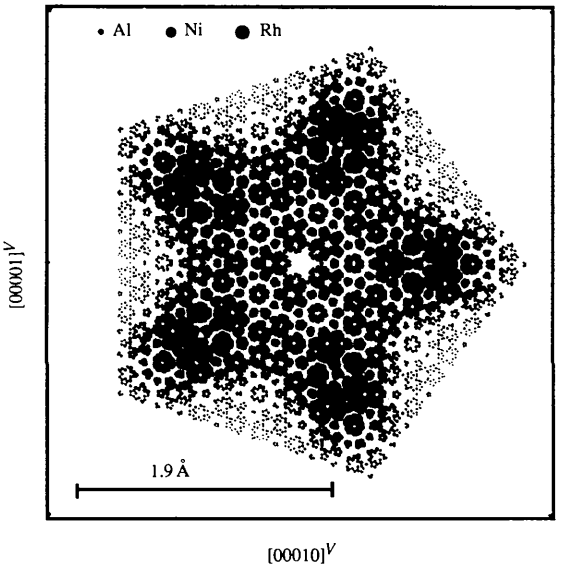

Fig. 3. Simulated structure: acceptance domain of hyperatom 1 based on a maximum-entropy calculation in $V^{\parallel}$ (760 × 760 Å) lifted in $V^{\perp}$ (cut-off limit: 1% ρ_{max}).

DESY. 5290 reflections were collected, of which 3725 were unique. Each peak was collected with its profile. A special background analysis was necessary as the data set was severely biased by diffuse scattering phenomena. Only reflections with $I > 8\sigma(I)$ showed reliable peak shapes, and these 790 reflections are used for the subsequent analysis.

Both the Patterson map (Fig. 4) and the corresponding symmetry minimum function (Fig. 5) were calculated on a 200×100 grid (0.04 Å per grid point) on the characteristic section spanned by $[11110]^D$ and $[00001]^D$. The symmetry minimum function was calculated in the plane group *p2mg*, which provides the symmetry of the characteristic section. Three corresponding Harker vectors $[2x_1, 2x_2]$, $[1/2, 2x_2]$ and $[2x_1 + 1/2, 0]$, neglecting the origin vector [00], were used. All maps are shown as contour plots with five equidistant levels between minimum and maximum values in that section. The correct positions of the hyperatoms related by permissible origin shifts are found within the topmost positions in the corresponding peak list. Obviously, despite the broad Patterson peaks, the symmetry minimum function generates a sharp map. The set of positions located at $[(2n-1) \times 0.2, 0, x_x, (2n-1) \times 0.2, 0]^V$ are incorrect. Referring to the plane group, these positions are related to the correct ones in $(2n \times 0.2, 0, x_3, 2n \times 0.2, 0)^V$ by an origin shift of $[\frac{1}{2}\ 0]$. Despite the fact that this origin shift is permissible in *p2mg* and no new information would be attained, there exists no analogous translation in the decagonal space group $P10_5/mmc$. Hence, two different decagonal structures would result. However, these peaks can be deferred by means of the embedding approach. The complete information of all possible positions of hyperatoms is obtained. The top two peaks of the symmetry minimum function were used as trial pivot elements for the image-seeking minimum function. Obviously, in both image-seeking minimum solutions, all hyperatoms are found (Fig. 6). The assignment of Al, Co and Ni to the hyperatoms was based on the weight of the corresponding peak. This model was taken as reliable electron-density distribution for fixing phases in the subsequent maximum-entropy analysis.

As in decagonal $Al_{70}Co_{15}Ni_{15}$ projecting the structure parallel to the periodic direction generates no overlap of the atomic positions, the maximum-entropy calculation can be reduced to a two-dimensional computation. As a first step, all structure factors $F(h_1, h_2, h_3, h_4, 0)$ were calculated based on the above crude model using simple pentagons as acceptance domains. Varying the shape and scattering power of the hyperatoms, a set of strong structure factors consisting of 14 reflections invariant under these operations could be separated and was fixed in the subsequent structure solution. The maximum-entropy method converged in 200 cycles from the trial electron density (the normalized Patterson map). All peaks were searched and their integral electron density was computed and the structure in physical space was then lifted into five dimensions and sections parallel to $V^\perp$ through the centres of the hyperatoms were drawn. For comparison, the structure as derived by modelling acceptance domains (Steurer *et al.*, 1993) and the *ab initio* solution using the procedure described above are shown (Fig. 7). The maximum-entropy solution shows impressively sharp acceptance domains with distinct subdivisions of different chemical composition. The innermost part (larger dots) represents the region occupied by transition metals. As can be seen by the fluent variation of the dot size, the outer part consisting mainly of aluminium comprises significant amounts of

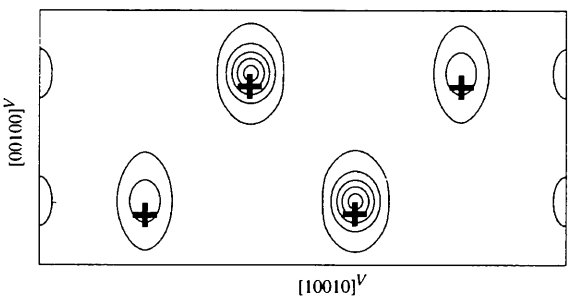

Fig. 5. $Al_{70}Co_{15}Ni_{15}$: characteristic section of the symmetry minimum function (SMF). The refined positions of the hyperatoms are marked for comparison.

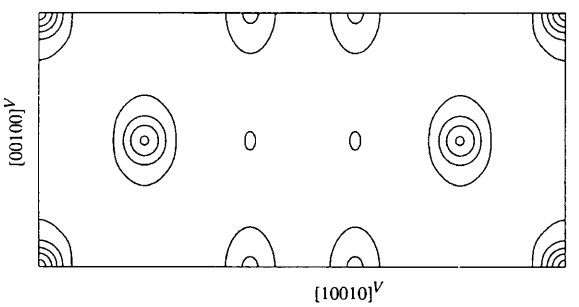

Fig. 4. $Al_{70}Co_{15}Ni_{15}$: characteristic section spanned by the periodic axis $[00001]^D$ and the diagonal of the hyperrhombohedric subcell $[11110]^D$ of the Patterson map.

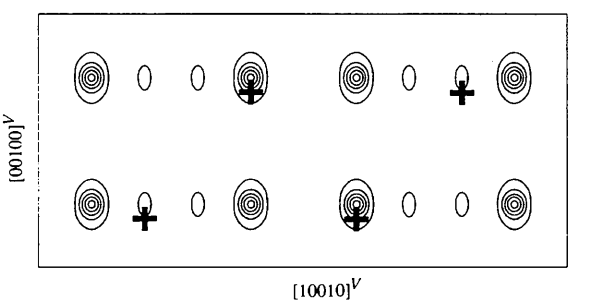

Fig. 6. $Al_{70}Co_{15}Ni_{15}$: characteristic section of the image-seeking minimum function (IMF). The refined positions of the hyperatoms are marked for comparison.

transition metals, which can be confirmed by the structure refinement. The structured distribution of the lifted atoms is induced by the limited size of the parallel-space region and has to be considered as homogeneously dense. Although the calculation was performed in perpendicular as well as in parallel space, parallel shifts of parts of the acceptance domains could not be found. However, there exists a significant amount of chemical and phason disorder (Haibach, Estermann, Steurer, Kalning & Kek, 1995).

Using the same procedure, the structure of decagonal $Al_{72}Fe_{23}Ni_5$ could be solved. The positions of the hyperatoms were retrieved by the SMF/IMF algorithm, whereas the shapes of the acceptance domains were found by the maximum-entropy method (Haibach, Steurer & Grushko, 1996).

5.2. *Structure of $Al_{70.5}Mn_{16.5}Pd_{13}$*

Decagonal $Al_{70.5}Mn_{16.5}Pd_{13}$ belongs to the family of quasicrystals with translation period of ~12 Å. A first crude structure model was proposed (Steurer, Haibach, Zhang, Beeli & Nissen, 1994) but a detailed structure model could not be derived since the analysis of the decagonal structure is severely biased by diffuse scattering. In consequence, the real structure would be considerably disordered and solving the average structure would be a rather large simplication. The X-ray data were collected using an Enraf–Nonius CAD-4 four-circle diffractometer. The five-dimensional unit-cell parameters were refined to $d_{1,\ldots,4} = 3.480\ (1)$, $d_5 = 12.557\ (1)$ Å, $\alpha_{ij} = 60$ and $\alpha_{i5} = 90°$ $(i, j = 1, \ldots, 4)$. Owing to systematic extinctions, the decagonal space group $P10_5/mmc$ has been selected. The data collection included 6647 reflections, of which 476 were unique, with $I > 3\sigma(I)$. The Patterson map (Fig. 8) was sampled on a grid 200 × 300 (0.04 Å per grid point). Again, the symmetry minimum function was calculated in the two-dimensional subgroup $p2mg$. For comparison with the structure solution, the final positions of the hyperatoms are indicated (Fig. 9). In contrast to the Patterson map, the SMF solution consists of very sharp peaks and all possible positions compatible with the space group can be found. For the same reasons mentioned in §5.1, a subset of peaks is deferred. With the first three peaks selected as pivot elements, a set of image-seeking minimum functions has been calculated. With only solutions in agreement with minimum bond lengths accepted, a trial structure model has been selected for a subsequent analysis with the maximum-entropy method (Fig. 10).

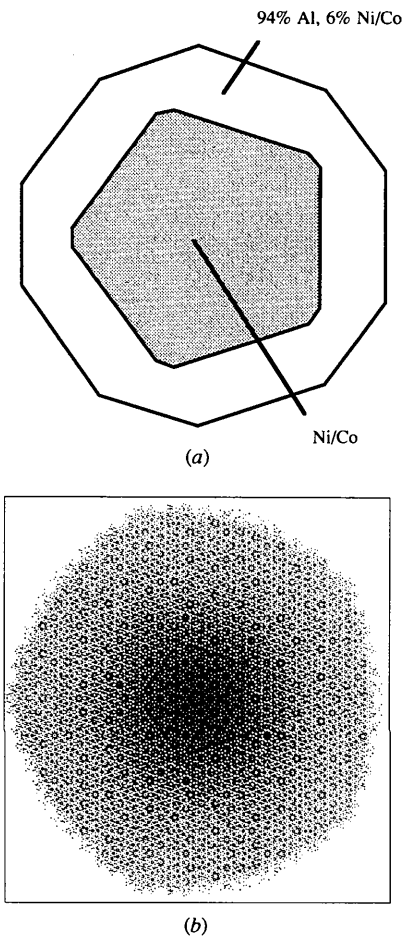

Fig. 7. $Al_{70}Co_{15}Ni_{15}$: (*a*) acceptance domain of hyperatom 1 as derived by modelling the acceptance domain; (*b*) acceptance domain of hyperatom 1 as obtained by the MEM.

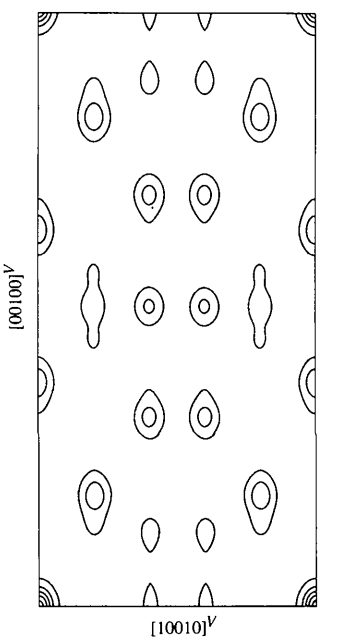

Fig. 8. $Al_{70.5}Mn_{16.5}Pd_{13}$: characteristic section spanned by the periodic axis $[00001]^D$ and the diagonal of the hyperrhombohedric subcell $[11110]^D$ of the Patterson map.

Contrary to the structure discussed in §5.1, different hyperatoms of $Al_{70.5}Mn_{16.5}Pd_{13}$ coincide if they are projected onto the decagonal plane. In consequence, the analysis with the maximum-entropy method was partitioned into two steps: (*a*) solving the projected structure, and (*b*) for computational reasons, retrieving the three-dimensional structure based on the preceding solution using a smaller box as parallel-space representation.

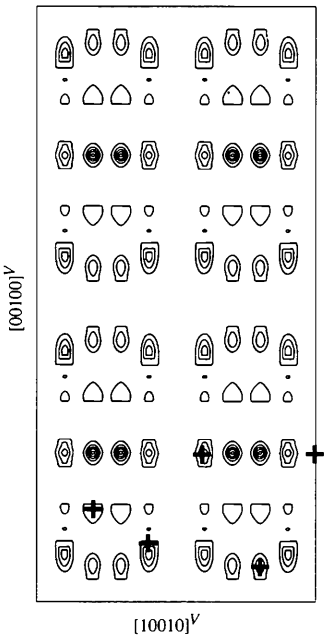

Fig. 9. $Al_{70.5}Mn_{16.5}Pd_{13}$: characteristic section of the symmetry minimum function. The refined positions of the hyperatoms are marked for comparison.

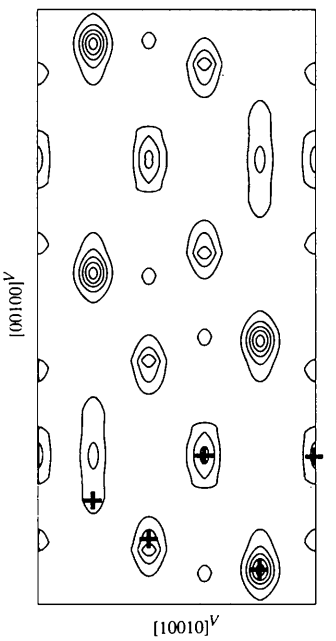

Fig. 10. $Al_{70.5}Mn_{16.5}Pd_{13}$: characteristic section of the image-seeking minimum function. The refined positions of the hyperatoms are marked for comparison.

The projected structure was determined fixing 23 structure factors being invariant when slightly modifying the SMF/IMF structure model. The calculation was performed on a 4000 × 4000 grid (0.19 Å per grid point) taking all symmety elements into account. All structure factors $F(h_1, h_2, h_3, h_4, 0)$ were obtained. The projected electron-density distribution (Fig. 11) was in accordance with models derived from HRTEM images (Beeli & Nissen, 1993).

For the subsequent analysis, the set of known structure factors was extended and a three-dimensional MEM map was computed starting from the projected electron-density distribution on a 1000 × 1000 × 80 grid and a corresponding volume of 195 × 195 × 12.557 Å^3. The final electron-density map was transformed into integrated densities and lifted into five dimensions. Special sections corresponding to the SMF/IMF solutions through the hyperatoms show the complicated boundaries and the different subdivisions of the acceptance domains (Fig. 12). As mentioned above, the distribution of the atoms in the acceptance domains is generated by the limited region lifted into $V^\perp$.

6. Concluding remarks

The efficiency of the combination of the symmetry minimum function and the maximum-entropy method in

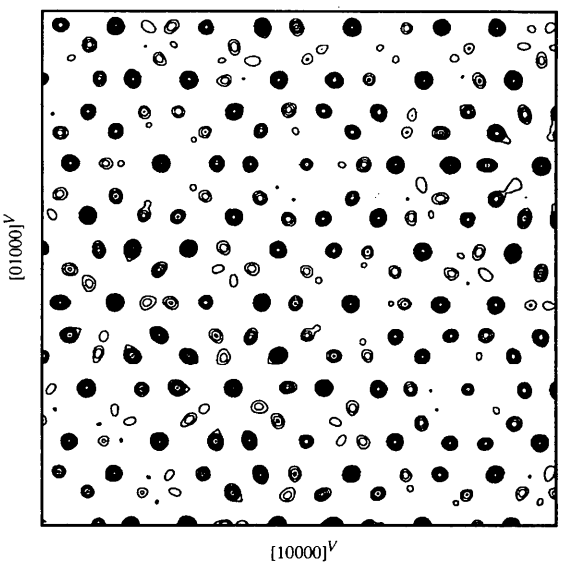

Fig. 11. $Al_{70.5}Mn_{16.5}Pd_{13}$: 23.4 × 23.4 Å region of the structure projected onto the quasiperiodic layer.

the n-dimensional description of quasicrystals was illustrated by two stucture determinations of decagonal quasicrystals with different complexity.

In the case of decagonal $Al_{70}Co_{15}Ni_{15}$, the previous structure determination could be improved and the acceptance domains could be described in more detail. As demonstrated with decagonal $Al_{70.5}Mn_{16.5}Pd_{13}$, the symmetry minimum function is a very powerful tool in deriving a first n-dimensional structure model constrained only to the corresponding space-group symmetry. Because the data sets are severely limited, the maximum-entropy method is the best way in further analysing the acceptance domains. Two different real-space approaches were presented. With a physical-space representation, the best results could be obtained and the acceptance domains could be solved by lifting the corresponding electron density into five dimensions.

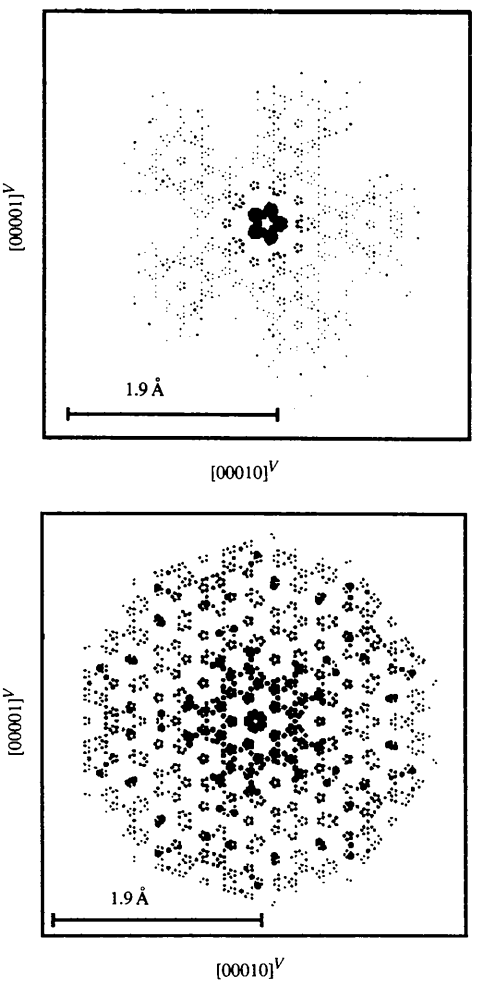

Fig. 12. $Al_{70}Mn_{16.5}Pd_{13}$: acceptance domains of hyperatom 1 and hyperatom 2 (Steurer *et al.*, 1994) obtained by lifting the three-dimensional MEM electron-density solution (cut-off limit: 1% ρ_{max}).

Both methods have not yet been tested with icosahedral quasicrystals, but it is expected that the symmetry minimum function and the maximum-entropy method in $V^\perp$ centred at the hyperatoms will solve these structures as well, while the use of the algorithm based on a representation in physical space will fail owing to the limited computing facilities available up to now.

All synchrotron experiments were performed at the HASYLAB synchrotron facility at DESY. The authors thank Stefan Kek for help in the measurements and Michael A. Estermann for many inspiring discussions.

References

Beeli, C. & Nissen, H.-U. (1993). *J. Non-Cryst. Solids*, **153/154**, 463–467.
deBoissieu, M., Stephens, P., Boudard, M., Janot, C., Chapman, D. L. & Audier, M. (1994). *Phys. Rev. Lett.* **72**, 3538–3541.
Bricogne, G. (1984). *Acta Cryst.* A**40**, 410–445.
Bricogne, G. (1993). *Acta Cryst.* D**49**, 37–60.
Collins, D. M. (1982). *Nature (London)*, 49–51.
Collins, D. M. & Mahar, M. C. (1983). *Acta Cryst.* A**39**, 252–256.
Estermann, M. A. (1995). *Nucl. Instrum. Methods*, **354**, 126–133.
Frey, F. & Steurer, W. (1993). *J. Non-Cryst. Solids*, **153/154**, 600–605.
Fu, Z., Li, F. & Fan, H. (1993). *Z. Kristallogr.* **190**, 57–68.
Haibach, T. (1994). PhD thesis, ETH Zurich, Switzerland.
Haibach, T., Estermann, M. A., Steurer, W., Kalning, M. & Kek, S. (1995). *Proceedings of the 5th International Conference on Quasicrystals (ICQ95)*. Singapore: World Scientific.
Haibach, T., Steurer, W. & Grushko, B. (1996). In preparation.
Harker, D. (1936). *J. Chem. Phys.* pp. 381–390.
Hirshfeld, F. L. (1968). *Acta Cryst.* A**24**, 301–311.
Janssen, T. (1988). *Phys. Rep.* **168**, 55–113.
Jaric, M. V. (1986). *Phys. Rev. B*, **34**, 4685–4698.
Jaric, M. V. & Qiu, S. Y. (1993). *Acta Cryst.* A**49**, 576–585.
Kalugin, P. A. & Katz, A. (1993). *Europhys. Lett.* **21**, 921–926.
Livesey, A. K. & Skilling, J. (1985). *Acta Cryst.* A**41**, 113–122.
Mermin, N. D. (1992). *Rev. Mod. Phys.* **64**, 3–49.
Papoular. R. J., deBoissieu, M. & Janot, C. (1991). *Methods of Structural Analysis of Modulated Structures and Quasicrystals*, edited by J. M. Pérez-Mato, F. J. Zúñiga & G. Madariaga, pp. 333–343. Singapore: World Scientific.
Sakata, M. & Sato, M. (1990). *Acta Cryst.* A**46**, 263–270.
Simpson, P. G., Dobrott, R. D. & Lipscomb, W. (1965). *Acta Cryst.* **18**, 169–179.
Steurer, W. (1989). *Acta Cryst.* B**45**, 534–542.
Steurer, W. (1991). *Methods of Structural Analysis of Modulated Structures and Quasicrystals*, edited by J. M. Pérez-Mato, F. J. Zúñiga & G. Madaraiga, pp. 344–349. Singapore: World Scientific.
Steurer, W., Haibach, T., Zhang, B., Beeli, C. & Nissen, H.-U. (1994). *J. Phys Condens. Matter*, **6**, 613–632.
Steurer, W., Haibach, T., Zhang, B., Kek, S. & Lück, R. (1993). *Acta Cryst.* B**49**, 661–675.